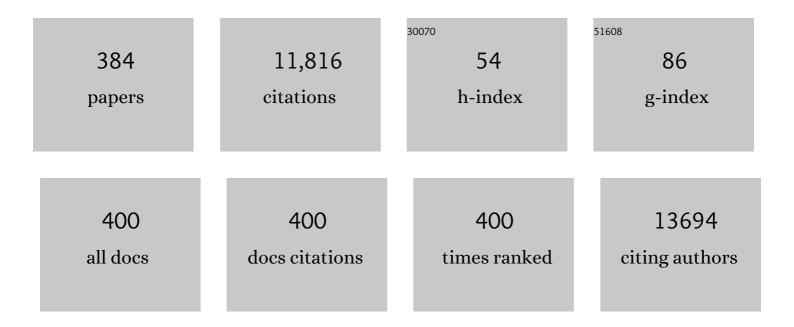
## Xiao-Ying Zhang

List of Publications by Year in descending order

Source: https://exaly.com/author-pdf/1439177/publications.pdf Version: 2024-02-01



#	Article	IF	CITATIONS
1	Highâ€Energy/Power and Lowâ€Temperature Cathode for Sodiumâ€Ion Batteries: In Situ XRD Study and Superior Fullâ€Cell Performance. Advanced Materials, 2017, 29, 1701968.	21.0	350
2	Palladium-Catalyzed Câ^'H Aminations of Anilides with <i>N</i> -Fluorobenzenesulfonimide. Journal of the American Chemical Society, 2011, 133, 1694-1697.	13.7	328
3	N-rich zeolite-like metal–organic framework with sodalite topology: high CO2 uptake, selective gas adsorption and efficient drug delivery. Chemical Science, 2012, 3, 2114.	7.4	277
4	Highly Regioselective Copper atalyzed Benzylic CH Amination by <i>N</i> â€Fluorobenzenesulfonimide. Angewandte Chemie - International Edition, 2012, 51, 1244-1247.	13.8	212
5	A Scalable Strategy To Develop Advanced Anode for Sodium-Ion Batteries: Commercial Fe <sub>3</sub> O <sub>4</sub> -Derived Fe <sub>3</sub> O <sub>4</sub> @FeS with Superior Full-Cell Performance. ACS Applied Materials & Interfaces, 2018, 10, 3581-3589.	8.0	209
6	Regioselective Radical Aminofluorination of Styrenes. Angewandte Chemie - International Edition, 2014, 53, 11079-11083.	13.8	200
7	Burnout and its association with resilience in nurses: A crossâ€sectional study. Journal of Clinical Nursing, 2018, 27, 441-449.	3.0	176
8	P2–Na <sub>2/3</sub> Ni <sub>1/3</sub> Mn <sub>5/9</sub> Al <sub>1/9</sub> O <sub>2</sub> Microparticles as Superior Cathode Material for Sodium-Ion Batteries: Enhanced Properties and Mechanism via Graphene Connection. ACS Applied Materials & Interfaces, 2016, 8, 20650-20659.	8.0	168
9	In Situ Binding Sb Nanospheres on Graphene via Oxygen Bonds as Superior Anode for Ultrafast Sodium-Ion Batteries. ACS Applied Materials & Interfaces, 2016, 8, 7790-7799.	8.0	167
10	A self-destructive nanosweeper that captures and clears amyloid β-peptides. Nature Communications, 2018, 9, 1802.	12.8	144
11	A Practicable Li/Naâ€ion Hybrid Full Battery Assembled by a Highâ€Voltage Cathode and Commercial Graphite Anode: Superior Energy Storage Performance and Working Mechanism. Advanced Energy Materials, 2018, 8, 1702504.	19.5	142
12	Nanoeffects promote the electrochemical properties of organic Na2C8H4O4 as anode material for sodium-ion batteries. Nano Energy, 2015, 13, 450-457.	16.0	139
13	Pseudocapacitance-boosted ultrafast Na storage in a pie-like FeS@C nanohybrid as an advanced anode material for sodium-ion full batteries. Nanoscale, 2018, 10, 9218-9225.	5.6	135
14	Advanced P2-Na <sub>2/3</sub> Ni <sub>1/3</sub> Mn <sub>7/12</sub> Fe <sub>1/12</sub> O <sub>2</sub> Cathode Material with Suppressed P2–O2 Phase Transition toward High-Performance Sodium-Ion Battery. ACS Applied Materials & Interfaces, 2018, 10, 34272-34282.	8.0	127
15	Highâ€Performance and Lowâ€Temperature Lithium–Sulfur Batteries: Synergism of Thermodynamic and Kinetic Regulation. Advanced Energy Materials, 2018, 8, 1703638.	19.5	124
16	Metastable Marcasite-FeS <sub>2</sub> as a New Anode Material for Lithium Ion Batteries: CNFs-Improved Lithiation/Delithiation Reversibility and Li-Storage Properties. ACS Applied Materials & Interfaces, 2017, 9, 10708-10716.	8.0	122
17	Host Materials Transformable in Tumor Microenvironment for Homing Theranostics. Advanced Materials, 2017, 29, 1605869.	21.0	121
18	Hollow Manganese Silicate Nanotubes with Tunable Secondary Nanostructures as Excellent Fentonâ€Type Catalysts for Dye Decomposition at Ambient Temperature. Advanced Functional Materials, 2016, 26, 7334-7342.	14.9	116

#	Article	IF	CITATIONS
19	Covalent Organic Framework with Highly Accessible Carbonyls and ï€â€Cation Effect for Advanced Potassiumâ€lon Batteries. Angewandte Chemie - International Edition, 2022, 61, .	13.8	112
20	Workplace violence against nurses: A cross-sectional study. International Journal of Nursing Studies, 2017, 72, 8-14.	5.6	111
21	Shale-like Co <sub>3</sub> O <sub>4</sub> for high performance lithium/sodium ion batteries. Journal of Materials Chemistry A, 2016, 4, 8242-8248.	10.3	108
22	Novel highly selective anion chemosensors based on 2,5-bis(2-hydroxyphenyl)-1,3,4-oxadiazole. Tetrahedron Letters, 2003, 44, 131-134.	1.4	105
23	Dual-Porosity SiO <sub>2</sub> /C Nanocomposite with Enhanced Lithium Storage Performance. Journal of Physical Chemistry C, 2015, 119, 3495-3501.	3.1	105
24	High rate capability and long-term cyclability of Li4Ti4.9V0.1O12 as anode material in lithium ion battery. Electrochimica Acta, 2011, 56, 8611-8617.	5.2	104
25	The Effective Design of a Polysulfide-Trapped Separator at the Molecular Level for High Energy Density Li–S Batteries. ACS Applied Materials & Interfaces, 2016, 8, 16108-16115.	8.0	103
26	Design of donors with broad absorption regions and suitable frontier molecular orbitals to match typical acceptors via substitution on oligo(thienylenevinylene) toward solar cells. Journal of Computational Chemistry, 2012, 33, 1353-1363.	3.3	99
27	An unusual ten-connected self-penetrating metal–organic framework based on tetranuclear cobalt clusters. Chemical Communications, 2010, 46, 8383.	4.1	94
28	Crossâ€Cycloaddition of Two Different Isocyanides: Chemoselective Heterodimerization and [3+2]â€Cyclization of 1,4â€Diazabutatriene. Angewandte Chemie - International Edition, 2016, 55, 7077-7080.	13.8	91
29	Boosting Polysulfide Redox Kinetics by Graphene‣upported Ni Nanoparticles with Carbon Coating. Advanced Energy Materials, 2020, 10, 2000907.	19.5	89
30	Anionic Lanthanide Metal–Organic Frameworks: Selective Separation of Cationic Dyes, Solvatochromic Behavior, and Luminescent Sensing of Co(II) Ion. Inorganic Chemistry, 2018, 57, 11463-11473.	4.0	88
31	Prevalence and related influencing factors of depressive symptoms for empty-nest elderly living in the rural area of YongZhou, China. Archives of Gerontology and Geriatrics, 2010, 50, 24-29.	3.0	87
32	Li <sub>3</sub> PO <sub>4</sub> â€Coated LiNi <sub>0.5</sub> Mn <sub>1.5</sub> O <sub>4</sub> : A Stable Highâ€Voltage Cathode Material for Lithiumâ€Ion Batteries. Chemistry - A European Journal, 2014, 20, 7479-7485.	3.3	87
33	Double [4 + 2] Cycloaddition Reaction To Approach a Large Acene with Even-Number Linearly Fused Benzene Rings: 6,9,16,19-Tetraphenyl-1.20,4.5,10.11,14.15-Tetrabenzooctatwistacene. Journal of Organic Chemistry, 2015, 80, 109-113.	3.2	86
34	Dual-carbon enhanced silicon-based composite as superior anode material for lithium ion batteries. Journal of Power Sources, 2016, 307, 738-745.	7.8	81
35	Supramolecular Nano-Aggregates Based on Bis(Pyrene) Derivatives for Lysosome-Targeted Cell Imaging. Journal of Physical Chemistry C, 2013, 117, 26811-26820.	3.1	79
36	Understanding the anchoring effect of Graphene, BN, C2N and C3N4 monolayers for lithiumâ^'polysulfides in Liâ^'S batteries. Applied Surface Science, 2018, 434, 596-603.	6.1	78

#	Article	IF	CITATIONS
37	Li-decorated porous graphene as a high-performance hydrogen storage material: A first-principles study. International Journal of Hydrogen Energy, 2017, 42, 10099-10108.	7.1	77
38	Quasi-Solid-State Sodium-Ion Full Battery with High-Power/Energy Densities. ACS Applied Materials & Interfaces, 2018, 10, 17903-17910.	8.0	74
39	Dual responsive supramolecular nanogels for intracellular drug delivery. Chemical Communications, 2014, 50, 3789.	4.1	70
40	Quantum Chemical Analysis of the Chemical Bonds in Tris(8-hydroxyquinolinato)aluminum as a Key Emitting Material for OLED. Journal of Physical Chemistry A, 2004, 108, 10296-10301.	2.5	69
41	Preparation and Crystal Structure of Dual-Functional Precursor Complex Bis(acetylacetonato)nickel(II) with 4-Pyridyltetrathiafulvalene. Inorganic Chemistry, 2006, 45, 6860-6863.	4.0	68
42	Adsorption of phosgene molecule on the transition metal-doped graphene: First principles calculations. Applied Surface Science, 2017, 425, 340-350.	6.1	67
43	A promising PMHS/PEO blend polymer electrolyte for all-solid-state lithium ion batteries. Dalton Transactions, 2018, 47, 14932-14937.	3.3	67
44	The effects of resilience and turnover intention on nurses' burnout: Findings from a comparative crossâ€sectional study. Journal of Clinical Nursing, 2019, 28, 499-508.	3.0	66
45	Spatial confinement of vertical arrays of lithiophilic SnS2 nanosheets enables conformal Li nucleation/growth towards dendrite-free Li metal anode. Energy Storage Materials, 2021, 36, 504-513.	18.0	66
46	Nanoscale Polysulfides Reactors Achieved by Chemical Au–S Interaction: Improving the Performance of Li–S Batteries on the Electrode Level. ACS Applied Materials & Interfaces, 2015, 7, 27959-27967.	8.0	65
47	Exploring resilience in Chinese nurses: a cross-sectional study. Journal of Nursing Management, 2017, 25, 223-230.	3.4	65
48	The First Nonthiolic, Odorless 1,3-Propanedithiol Equivalent and Its Application in Thioacetalization. Journal of Organic Chemistry, 2003, 68, 9148-9150.	3.2	63
49	Target construction of ultrathin graphitic carbon encapsulated FeS hierarchical microspheres featuring superior low-temperature lithium/sodium storage properties. Journal of Materials Chemistry A, 2018, 6, 7997-8005.	10.3	62
50	Co <sub>3</sub> O <sub>4</sub> Nanospheres Embedded in a Nitrogen-Doped Carbon Framework: An Electrode with Fast Surface-Controlled Redox Kinetics for Lithium Storage. ACS Energy Letters, 2017, 2, 52-59.	17.4	61
51	Water-Robust Zinc–Organic Framework with Mixed Nodes and Its Handy Mixed-Matrix Membrane for Highly Effective Luminescent Detection of Fe <sup>3+</sup> , CrO <sub>4</sub> <sup>2–</sup> , and Cr <sub>2</sub> O <sub>7</sub> <sup>2–</sup> in Aqueous Solution. Inorganic Chemistry, 2021, 60, 1716-1725.	4.0	61
52	Oxygenâ€Deficient Titanium Dioxide Nanosheets as More Effective Polysulfide Reservoirs for Lithiumâ€Sulfur Batteries. Chemistry - A European Journal, 2017, 23, 9666-9673.	3.3	60
53	A Novel Layered Sedimentary Rocks Structure of the Oxygen-Enriched Carbon for Ultrahigh-Rate-Performance Supercapacitors. ACS Applied Materials & Interfaces, 2016, 8, 4233-4241.	8.0	58
54	Naphthyl and Thionaphthyl Endâ€Capped Oligothiophenes as Organic Semiconductors: Effect of Chain Length and Endâ€Capping Groups. Advanced Functional Materials, 2007, 17, 1940-1951.	14.9	57

#	Article	IF	CITATIONS
55	A biomimetic platelet based on assembling peptides initiates artificial coagulation. Science Advances, 2020, 6, eaaz4107.	10.3	56
56	Radical Mechanism of Isocyanide-Alkyne Cycloaddition by Multicatalysis of Ag2CO3, Solvent, and Substrate. ACS Catalysis, 2015, 5, 6177-6184.	11.2	54
57	Three-dimensional carbon nanotube networks enhanced sodium trimesic: a new anode material for sodium ion batteries and Na-storage mechanism revealed by ex situ studies. Journal of Materials Chemistry A, 2017, 5, 16622-16629.	10.3	54
58	An FeP@C nanoarray vertically grown on graphene nanosheets: an ultrastable Li-ion battery anode with pseudocapacitance-boosted electrochemical kinetics. Nanoscale, 2019, 11, 1304-1312.	5.6	53
59	Bis-pyrene-based supramolecular aggregates with reversibly mechanochromic and vapochromic responsiveness. Journal of Materials Chemistry C, 2014, 2, 1887.	5.5	52
60	Polyvinylpyrrolidone (PVP) assisted synthesized nano-LiFePO4/C composite with enhanced low temperature performance. Electrochimica Acta, 2013, 97, 92-98.	5.2	51
61	Study on a highly selective fluorescent chemosensor for Fe3+ based on 1,3,4-oxadiazole and phosphonic acid. Sensors and Actuators B: Chemical, 2014, 200, 259-268.	7.8	51
62	A new strategy for developing superior electrode materials for advanced batteries: using a positive cycling trend to compensate the negative one to achieve ultralong cycling stability. Nanoscale Horizons, 2016, 1, 496-501.	8.0	51
63	Multiple heterointerfaces boosted de-/sodiation kinetics towards superior Na storage and Na-Ion full battery. Journal of Materials Chemistry A, 2018, 6, 6578-6586.	10.3	50
64	Intracellular pH-Sensitive Metallo-Supramolecular Nanogels for Anticancer Drug Delivery. ACS Applied Materials & Interfaces, 2014, 6, 7816-7822.	8.0	49
65	Synergistic mediation of sulfur conversion in lithium–sulfur batteries by a Gerber tree-like interlayer with multiple components. Journal of Materials Chemistry A, 2017, 5, 11255-11262.	10.3	49
66	Rational Design of Organic Asymmetric Donors D1–A–D2 Possessing Broad Absorption Regions and Suitable Frontier Molecular Orbitals to Match Typical Acceptors toward Solar Cells. Journal of Physical Chemistry A, 2011, 115, 5184-5191.	2.5	48
67	2D few-layer iron phosphosulfide: a self-buffer heterophase structure induced by irreversible breakage of P–S bonds for high-performance lithium/sodium storage. Journal of Materials Chemistry A, 2019, 7, 1529-1538.	10.3	48
68	"CHâ€∕N Substitutedmer-Gaq3 andmer-Alq3 Derivatives: An Effective Approach for the Tuning of Emitting Color. Journal of Physical Chemistry B, 2005, 109, 17762-17767.	2.6	47
69	Intramolecular Azaâ€Antiâ€Michael Addition of an Amide Anion to Enones: A Regiospecific Approach to Tetramic Acid Derivatives. Advanced Synthesis and Catalysis, 2007, 349, 2301-2306.	4.3	47
70	A vertical and cross-linked Ni(OH) <sub>2</sub> network on cellulose-fiber covered with graphene as a binder-free electrode for advanced asymmetric supercapacitors. Journal of Materials Chemistry A, 2015, 3, 19077-19084.	10.3	47
71	Geometry and stability of fullerene cages: C24 to C70. International Journal of Quantum Chemistry, 2005, 105, 142-147.	2.0	44
72	Carbon/Binderâ€Free NiO@NiO/NF with In Situ Formed Interlayer for Highâ€Arealâ€Capacity Lithium Storage. Advanced Energy Materials, 2019, 9, 1803690.	19.5	44

#	Article	IF	CITATIONS
73	Shedding light on octathio[8]circulene and some of its plate-like derivatives. Physical Chemistry Chemical Physics, 2008, 10, 1743.	2.8	43
74	Organocatalyzed Anion Relay Leading to Functionalized 2,3-Dihydrofurans. Organic Letters, 2013, 15, 3978-3981.	4.6	43
75	<i>N</i> -Bromosuccinimide/1,8-Diazabicyclo[5.4.1]undec-7-ene Combination: β-Amination of Chalcones via a Tandem Bromoamination/Debromination Sequence. Organic Letters, 2013, 15, 852-855.	4.6	43
76	Assembly of MnCO 3 nanoplatelets synthesized at low temperature on graphene to achieve anode materials with high rate performance for lithium-ion batteries. Electrochimica Acta, 2016, 215, 267-275.	5.2	43
77	Optical Properties of the Phosphorescent Trinuclear Copper(I) Complexes of Pyrazolates:  Insights from Theory. Journal of Physical Chemistry A, 2007, 111, 4965-4973.	2.5	42
78	Egg yolk-derived carbon: Achieving excellent fluorescent carbon dots and high performance lithium-ion batteries. Journal of Alloys and Compounds, 2018, 746, 567-575.	5.5	42
79	Al doped MoS2 monolayer: A promising low-cost single atom catalyst for CO oxidation. Applied Surface Science, 2019, 484, 1297-1303.	6.1	42
80	Accurate Computation of Gas Uptake in Microporous Organic Molecular Crystals. Journal of Physical Chemistry C, 2012, 116, 8865-8871.	3.1	41
81	From Molecules to Materials: Molecular and Crystal Engineering Design of Organic Optoelectronic Functional Materials for High Carrier Mobility. Journal of Physical Chemistry C, 2012, 116, 1195-1199.	3.1	41
82	Three novel 1D lanthanide-carboxylate polymeric complexes: syntheses, crystal structures and magnetic analyses. Dalton Transactions, 2013, 42, 8504.	3.3	41
83	Alkyne aminohalogenation enabled by DBU-activated N-haloimides: direct synthesis of halogenated enamines. Chemical Communications, 2014, 50, 2360.	4.1	41
84	Full Protection for Graphene-Incorporated Micro-/Nanocomposites Containing Ultra-small Active Nanoparticles: the Best Li-Storage Properties. Particle and Particle Systems Characterization, 2015, 32, 1020-1027.	2.3	41
85	pH-responsive metallo-supramolecular nanogel for synergistic chemo-photodynamic therapy. Acta Biomaterialia, 2015, 25, 162-171.	8.3	41
86	Do the bridging oxygen bonds between active Sn nanodots and graphene improve the Li-storage properties?. Energy Storage Materials, 2016, 5, 214-222.	18.0	41
87	Electric-field controlled capture or release of phosgene molecule on graphene-based materials: First principles calculations. Applied Surface Science, 2018, 427, 1019-1026.	6.1	41
88	X-Shaped donor molecules based on benzo[2,1-b:3,4-b′]dithiophene as organic solar cell materials with PDIs as acceptors. Journal of Materials Chemistry A, 2013, 1, 13828.	10.3	40
89	Layered g-C <sub>3</sub> N <sub>4</sub> @Reduced Graphene Oxide Composites as Anodes with Improved Rate Performance for Lithium-Ion Batteries. ACS Applied Materials & Interfaces, 2018, 10, 30330-30336.	8.0	40
90	The in-situ-prepared micro/nanocomposite composed of Sb and reduced graphene oxide as superior anode for sodium-ion batteries. Journal of Alloys and Compounds, 2016, 672, 72-78.	5.5	39

#	Article	lF	CITATIONS
91	Synthesis and Characterization of Monodisperse Oligo(fluorene-co-bithiophene)s. Chemistry - A European Journal, 2007, 13, 6238-6248.	3.3	38
92	Push–pull effect on the charge transfer, and tuning of emitting color for disubstituted derivatives of mer-Alq3. Chemical Physics, 2009, 364, 39-45.	1.9	38
93	Investigation of twoâ€dimensional hfâ€based MXenes as the anode materials for li/naâ€ion batteries: A DFT study. Journal of Computational Chemistry, 2019, 40, 1352-1359.	3.3	38
94	Quantum chemical analysis of the chemical bonds in Mq3 (M=AlIII, GaIII) as emitting material for OLED. Chemical Physics Letters, 2004, 394, 120-125.	2.6	37
95	Metal-Dependent Assembly of a Helical-[Co3L3] Cluster versus a Meso-[Cu2L2] Cluster with O,N,N′,O′-Schiff Base Ligand: Structures and Magnetic Properties. Inorganic Chemistry, 2008, 47, 10317-10324.	4.0	37
96	Fluorinated derivatives of mer-Alq3: energy decomposition analysis, optical properties, and charge transfer study. Theoretical Chemistry Accounts, 2009, 122, 275-281.	1.4	37
97	gem-Dialkylthio vinylallenes: alkylthio-regulated reactivity and application in the divergent synthesis of pyrroles and thiophenes. Chemical Communications, 2012, 48, 8802.	4.1	37
98	A novel approach to prepare Si/C nanocomposites with yolk–shell structures for lithium ion batteries. RSC Advances, 2014, 4, 36218-36225.	3.6	37
99	An Efficient Strategy for Self-Assembly of DNA-Mimic Homochiral 1D Helical Cu(II) Chain from Achiral Flexible Ligand by Spontaneous Resolution. Inorganic Chemistry, 2016, 55, 3378-3383.	4.0	37
100	Selfâ€Assembled Fluorescent Organic Nanomaterials for Biomedical Imaging. Advanced Healthcare Materials, 2018, 7, e1800344.	7.6	37
101	A rational design strategy for donors in organic solar cells: the conjugated planar molecules possessing anisotropic multibranches and intramolecular charge transfer. Journal of Materials Chemistry, 2011, 21, 11159.	6.7	36
102	(PO4)3â^' polyanions doped LiNi1/3Co1/3Mn1/3O2: An ultrafast-rate, long-life and high-voltage cathode material for Li-ion rechargeable batteries. Electrochimica Acta, 2016, 201, 8-19.	5.2	36
103	Porous Carbon with Willow-Leaf-Shaped Pores for High-Performance Supercapacitors. ACS Applied Materials & Interfaces, 2017, 9, 42699-42707.	8.0	36
104	Charge Transport Parameters and Structural and Electronic Properties of Octathio[8]circulene and Its Plate-like Derivatives. Journal of Physical Chemistry A, 2009, 113, 255-262.	2.5	35
105	Understanding the electrochemical properties of A <sub>2</sub> MSiO <sub>4</sub> (A = Li and Na; M =) Tj ETC calculations. Journal of Materials Chemistry A, 2016, 4, 17455-17463.	Qq1 1 0.78 10.3	34314 rgBT ( 35
106	Tailoring Coral-Like Fe <sub>7</sub> Se <sub>8</sub> @C for Superior Low-Temperature Li/Na-Ion Half/Full Batteries: Synthesis, Structure, and DFT Studies. ACS Applied Materials & amp; Interfaces, 2019, 11, 47886-47893.	8.0	35
107	Pseudocapacitive sodium storage of Fe1â^'xS@N-doped carbon for low-temperature operation. Science China Materials, 2020, 63, 505-515.	6.3	35
108	A New Multifunctional Zinc–Organic Framework with Rare Interpenetrated Tripillared Bilayers as a Luminescent Probe for Detecting Ni <sup>2+</sup> and PO <sub>4</sub> <sup>3–</sup> in Water. Crystal Growth and Design, 2020, 20, 5120-5128.	3.0	35

#	Article	IF	CITATIONS
109	Polarity-Reversible Conjugate Addition Tuned by Remote Electronic Effects. Organic Letters, 2010, 12, 244-247.	4.6	34
110	Recent advances of transformable nanoparticles for theranostics. Chinese Chemical Letters, 2017, 28, 1808-1816.	9.0	34
111	Bipyridyl Second Ligand Dependent Structural and Magnetic Properties of Cu(II) Complexes with Pyridine-2,6-dicarboxylate and Water Molecule as First Ligand. Crystal Growth and Design, 2008, 8, 3803-3809.	3.0	33
112	LiV <sub>3</sub> O <sub>8</sub> nanorods as cathode materials for high-power and long-life rechargeable lithium-ion batteries. RSC Advances, 2014, 4, 25494-25501.	3.6	33
113	Improve the Overall Performances of Lithium Ion Batteries by a Facile Method of Modifying the Surface of Cu Current Collector with Carbon. Electrochimica Acta, 2015, 176, 604-609.	5.2	33
114	Freestanding Na <sub>3</sub> V <sub>2</sub> O <sub>2</sub> (PO <sub>4</sub> ) <sub>2</sub> F/Graphene Aerogels as High-Performance Cathodes of Sodium-Ion Full Batteries. ACS Applied Materials & Interfaces, 2020, 12, 41419-41428.	8.0	33
115	Heteroatom-Substituted Expanded Radialenes:Â One-Pot Synthesis and Characterization of Expanded 1,3-Dithiolane[n]radialenes. Journal of Organic Chemistry, 2005, 70, 6913-6917.	3.2	32
116	Positive psychotherapy for depression and selfâ€efficacy in undergraduate nursing students: A randomized, controlled trial. International Journal of Mental Health Nursing, 2017, 26, 375-383.	3.8	32
117	Hypervalent iodine(iii)-mediated cyclopropa(e)nation of alkenes/alkynes under mild conditions. Organic and Biomolecular Chemistry, 2014, 12, 1341.	2.8	31
118	Colloidal synthesis of greigite nanoplates with controlled lateral size for electrochemical applications. Nanoscale, 2015, 7, 4171-4178.	5.6	31
119	Catalytic CO oxidation by Fe doped penta-graphene: A density functional study. Molecular Catalysis, 2019, 470, 48-55.	2.0	31
120	Three-dimensional hierarchical Ni <sub>3</sub> Se <sub>2</sub> nanorod array as binder/carbon-free electrode for high-areal-capacity Na storage. Nanoscale, 2018, 10, 18942-18948.	5.6	30
121	Design of Tetrathiafulvalene-Based Phosphazenes Combining a Good Electron-Donor Capacity and Possible Inclusion Adduct Formation (Part II). Journal of Physical Chemistry C, 2007, 111, 4838-4846.	3.1	29
122	Effect of one ligand substitution on charge transfer and optical properties in mer-Alq3: a theoretical study. Theoretical Chemistry Accounts, 2009, 124, 339-344.	1.4	29
123	Synergistic Design of Cathode Region for the High-Energy-Density Li–S Batteries. ACS Applied Materials & Interfaces, 2016, 8, 28689-28699.	8.0	29
124	Diverse Structures Based on a Heptanuclear Cobalt Cluster with 0D to 3D Metal–Organic Frameworks: Magnetism and Application in Batteries. Chemistry - A European Journal, 2018, 24, 1962-1970.	3.3	29
125	Theoretical investigations of the charge transfer properties of anthracene derivatives. Theoretical Chemistry Accounts, 2010, 127, 587-594.	1.4	28
126	Mechanistic and Kinetic Study of CF <sub>3</sub> CHâ•€H <sub>2</sub> + OH Reaction. Journal of Physical Chemistry A, 2012, 116, 3172-3181.	2.5	28

#	Article	IF	CITATIONS
127	Rational design of phenoxazine-based donor–acceptor–donor thermally activated delayed fluorescent molecules with high performance. Physical Chemistry Chemical Physics, 2015, 17, 20014-20020.	2.8	28
128	Ground- and Excited-State Proton Transfer and Rotamerism in 2-(2-Hydroxyphenyl)-5-phenyl-1,3,4-oxadiazole and Its O/"NH or S―Substituted Derivatives. Journal of Physical Chemistry A, 2007, 111, 6354-6360.	2.5	27
129	Depression of Chronic Medical Inpatients in China. Archives of Psychiatric Nursing, 2008, 22, 39-49.	1.4	27
130	Packing Effect on the Transfer Integrals and Mobility in α,α′-bis(dithieno[3,2-b:2′,3′-d]thiophene) (BDT) its Heteroatom-Substituted Analogues. Australian Journal of Chemistry, 2011, 64, 1587.	and 0.9	27
131	Mechanistic understanding of domino cyclization between gem-dialkylthio vinylallenes and benzylamine towards economic synthesis: a computational study. Green Chemistry, 2014, 16, 2653.	9.0	27
132	Enhancement of electrochemical performance of LiNi1/3Co1/3Mn1/3O2 by surface modification with MnO2. Journal of Alloys and Compounds, 2015, 651, 12-18.	5.5	27
133	Porous Amorphous Co <sub>2</sub> P/N,B oâ€doped Carbon Composite as an Improved Anode Material for Sodiumâ€ion Batteries. ChemElectroChem, 2017, 4, 1395-1401.	3.4	27
134	Decametallic Co <sup>II</sup> lusterâ€Based Microporous Magnetic Framework with a Semirigid Multicoordinating Ligand. Chemistry - A European Journal, 2013, 19, 5097-5103.	3.3	26
135	Carbon-Free Porous Zn <sub>2</sub> GeO <sub>4</sub> Nanofibers as Advanced Anode Materials for High-Performance Lithium Ion Batteries. ACS Applied Materials & Interfaces, 2016, 8, 31722-31728.	8.0	26
136	Fabrication of boron-doped porous carbon with termite nest shape via natural macromolecule and borax to obtain lithium-sulfur/sodium-ion batteries with improved rate performance. Electrochimica Acta, 2017, 244, 86-95.	5.2	26
137	Understanding the rise of <i>Yinao</i> in China: A commentary on the little known phenomenon of healthcare violence. Australian Journal of Cancer Nursing, 2017, 19, 183-187.	1.6	26
138	Benign Recycling of Spent Batteries towards Allâ€Solidâ€State Lithium Batteries. Chemistry - A European Journal, 2019, 25, 8975-8981.	3.3	26
139	Using triazine as coupling unit for intra and intermolecular ferromagnetic coupling I. Chemical Physics, 1997, 214, 291-299.	1.9	25
140	Computational study on optical and electronic properties of the "CH″N substituted emitting materials based on spirosilabifluorene derivatives. Computational and Theoretical Chemistry, 2008, 862, 85-91.	1.5	25
141	Theoretical Study on the Gas Phase Reaction of Allyl Alcohol with Hydroxyl Radical. Journal of Physical Chemistry A, 2013, 117, 6629-6640.	2.5	25
142	Otherwise inert reaction of sulfonamides/carboxamides with formamides via proton transfer-enhanced reactivity. Organic and Biomolecular Chemistry, 2013, 11, 2460.	2.8	25
143	A WeChatâ€based "Three Good Things―positive psychotherapy for the improvement of job performance and selfâ€efficacy in nurses with burnout symptoms: A randomized controlled trial. Journal of Nursing Management, 2020, 28, 480-487.	3.4	25
144	Fe doped BN monolayer: A promising low-cost single atom catalyst for promoted CO oxidation activity. Applied Surface Science, 2020, 525, 146567.	6.1	25

#	Article	IF	CITATIONS
145	Tuning the electrochemical performance of Ti <sub>3</sub> C <sub>2</sub> and Hf <sub>3</sub> C <sub>2</sub> monolayer by functional groups for metal-ion battery applications. Nanoscale, 2021, 13, 11534-11543.	5.6	25
146	Theoretical investigations of the charge transfer characteristics in dichlorotitanium phthalocyanine (TiCl2Pc) and tin phthalocyanine (SnPc). Chemical Physics Letters, 2009, 483, 143-146.	2.6	24
147	D5hC50X10: Saturn-like fullerene derivatives (X=F, Cl, Br). Journal of Chemical Physics, 2005, 123, 094305.	3.0	23
148	Design of an Organic Zeolite toward the Selective Adsorption of Small Molecules at the Dispersion Corrected Density Functional Theory Level. Journal of Physical Chemistry B, 2009, 113, 16472-16478.	2.6	23
149	Catalysis in the Oil Droplet/Water Interface for Aromatic Claisen Rearrangement. Journal of Physical Chemistry A, 2010, 114, 4325-4333.	2.5	23
150	2D Fe <sub>2</sub> O <sub>3</sub> nanosheets with bi-continuous pores inherited from Fe-MOF precursors: an advanced anode material for Li-ion half/full batteries. 2D Materials, 2019, 6, 045022.	4.4	23
151	Turn-on fluorescence in a stable Cd(II) metal-organic framework for highly sensitive detection of Cr3+ in water. Dyes and Pigments, 2020, 178, 108359.	3.7	23
152	Crossâ€Cycloaddition of Two Different Isocyanides: Chemoselective Heterodimerization and [3+2]â€Cyclization of 1,4â€Diazabutatriene. Angewandte Chemie, 2016, 128, 7193-7196.	2.0	22
153	High performance LiNi <sub>0.5</sub> Mn <sub>1.5</sub> O <sub>4</sub> cathode material with a bi-functional coating for lithium ion batteries. RSC Advances, 2016, 6, 19245-19251.	3.6	22
154	Effective Cathode Design of Three-Layered Configuration for High-Energy Li–S Batteries. ACS Applied Materials & Interfaces, 2018, 10, 509-516.	8.0	22
155	A self-assembling peptide targeting VEGF receptors to inhibit angiogenesis. Chinese Chemical Letters, 2020, 31, 3153-3157.	9.0	22
156	An efficient theoretical study on host–guest interactions of a fluoride chemosensor with Fâ^', Clâ^' and Brâ~'. Chemical Physics, 2006, 331, 159-163.	1.9	21
157	Theoretical investigation on the white-light emission from a single-polymer system with simultaneous blue and orange emission (Part II). European Polymer Journal, 2011, 47, 208-224.	5.4	21
158	A plum-pudding like mesoporous SiO <sub>2</sub> /flake graphite nanocomposite with superior rate performance for LIB anode materials. Physical Chemistry Chemical Physics, 2015, 17, 22893-22899.	2.8	21
159	Flexible paper electrodes constructed from Zn <sub>2</sub> GeO <sub>4</sub> nanofibers anchored with amorphous carbon for advanced lithium ion batteries. Journal of Materials Chemistry A, 2016, 4, 2055-2059.	10.3	21
160	Broken symmetry approach and density functional theory calculations for heterospin system consisting of copper(II) and aminoxyl radicals. Chemical Physics, 2006, 330, 82-89.	1.9	20
161	Tuning the interactions from antiferro- to ferro-magnetic by molecular tailoring and manipulating. Dalton Transactions, 2013, 42, 3308-3317.	3.3	20
162	Divergent Reactions between αâ€Imino Rhodium Carbenoids and 1,3â€Diketones: Substrateâ€Controlled O–H versus C–H Insertion, European Journal of Organic Chemistry, 2017, 2017, 1289-1293	2.4	20

#	Article	IF	CITATIONS
163	Electrochemical In Situ Formation of a Stable Tiâ€Based Skeleton for Improved Liâ€Storage Properties: A Case Study of Porous CoTiO <sub>3</sub> Nanofibers. Chemistry - A European Journal, 2017, 23, 8712-8718.	3.3	20
164	Interface Water Catalysis of the Epoxide Opening. ChemPhysChem, 2010, 11, 65-69.	2.1	19
165	Electronic, optical and charge transfer properties of α,α′-bis(dithieno[3,2-b:2′,3′- d]thiophene) (BDT) an heteroatom-substituted analogues. Computational and Theoretical Chemistry, 2011, 968, 8-11.	d its 2.5	19
166	Fabrication of functionalized polysulfide reservoirs from large graphene sheets to improve the electrochemical performance of lithium–sulfur batteries. Physical Chemistry Chemical Physics, 2015, 17, 23481-23488.	2.8	19
167	Layer-stacked Sb@graphene micro/nanocomposite with decent Na-storage, full-cell and low-temperature performances. Journal of Alloys and Compounds, 2018, 731, 881-888.	5.5	19
168	An evaluation of a positive psychological intervention to reduce burnout among nurses. Archives of Psychiatric Nursing, 2019, 33, 186-191.	1.4	19
169	AgN <sub>3</sub> -Catalyzed Hydroazidation of Terminal Alkynes and Mechanistic Studies. Journal of the American Chemical Society, 2020, 142, 7083-7091.	13.7	19
170	Target encapsulating NiMoO4 nanocrystals into 1D carbon nanofibers as free-standing anode material for lithium-ion batteries with enhanced cycle performance. Journal of Alloys and Compounds, 2020, 830, 154648.	5.5	19
171	Engineering Allâ€Purpose Amorphous Carbon Nanotubes with High N/Oâ€Coâ€Doping Content to Bridge the Alkaliâ€Ion Batteries and Li Metal Batteries. Small, 2021, 17, e2006566.	10.0	19
172	Theoretical investigation on the white-light emission from a single-polymer system with simultaneous blue and orange emission. Polymer, 2009, 50, 6172-6185.	3.8	18
173	Morphology and surface properties of LiVOPO <sub>4</sub> : a first principles study. Physical Chemistry Chemical Physics, 2014, 16, 24604-24609.	2.8	18
174	Tuning the color of thermally activated delayed fluorescent properties for spiro-acridine derivatives by structural modification of the acceptor fragment: a DFT study. RSC Advances, 2015, 5, 18588-18592.	3.6	18
175	Alkaliâ€Metalâ€Ionâ€Functionalized Graphene Oxide as a Superior Anode Material for Sodiumâ€Ion Batteries. Chemistry - A European Journal, 2016, 22, 8152-8157.	3.3	18
176	Charge transfer NIR dyes for improved photoacoustic effect. Dyes and Pigments, 2016, 125, 392-398.	3.7	18
177	3D Hierarchical Microballs Constructed by Intertwined MnO@Nâ€doped Carbon Nanofibers towards Superior Lithiumâ€Storage Properties. Chemistry - A European Journal, 2018, 24, 9606-9611.	3.3	18
178	Molecular geometry, electronic structure and optical properties study of meridianal tris(8-hydroxyquinolinato)gallium(III) with ab initio and DFT methods. Computational and Theoretical Chemistry, 2005, 755, 19-30.	1.5	17
179	Theoretical study of chemosensor for fluoride and phosphate anions and optical properties of the derivatives of 2-(2-hydroxyphenyl)-1,3,4-oxadiazole. Chemical Physics, 2011, 380, 17-23.	1.9	17
180	Benzothienobenzothiophene-Based Conjugated Oligomers as Semiconductors for Stable Organic Thin-Film Transistors. ACS Applied Materials & Interfaces, 2014, 6, 5255-5262.	8.0	17

#	Article	IF	CITATIONS
181	The effect of high blood pressure-health literacy, self-management behavior, self-efficacy and social support on the health-related quality of life of Kazakh hypertension patients in a low-income rural area of China: a structural equation model. BMC Public Health, 2021, 21, 1114.	2.9	17
182	A Porous Metal–Organic Framework as an Electrochemical Sensing Platform for Highly Selective Adsorption and Detection of Bisphenols. Inorganic Chemistry, 2021, 60, 12049-12058.	4.0	17
183	Novel supramolecular architecture of high-spin aggregates? The comparison of ferromagnetic coupling through space and through hydrogen bond. Chemical Physics, 1997, 222, 1-7.	1.9	16
184	Theoretical study on C32 fullerenes and derivatives. Chemical Physics Letters, 2006, 428, 148-151.	2.6	16
185	Structural and magnetic properties of one-dimensional polymeric CoII complexes. Polyhedron, 2008, 27, 671-678.	2.2	16
186	Explaining the HOMO and LUMO distribution on individual ligands in mer-Alq3 and its "CHâ€∤N substituted derivatives. Computational and Theoretical Chemistry, 2008, 850, 79-83.	1.5	16
187	3 D Porous CoS <sub>2</sub> Hexadecahedron Derived from MOC toward Ultrafast and Longâ€Lifespan Lithium Storage. Chemistry - A European Journal, 2018, 24, 6798-6803.	3.3	16
188	Dual arbon Enhanced FeP Nanorods Vertically Grown on Carbon Nanotubes with Pseudocapacitanceâ€Boosted Electrochemical Kinetics for Superior Lithium Storage. Advanced Electronic Materials, 2019, 5, 1900006.	5.1	16
189	Revealing the potential application of chiral covalent organic frameworks in CO <sub>2</sub> adsorption and separation. New Journal of Chemistry, 2020, 44, 95-101.	2.8	16
190	How does the active site in the MoSe2 surface affect its electrochemical performance as anode material for metal-ion batteries?. Applied Surface Science, 2020, 526, 146637.	6.1	16
191	X―and H‧hape Two Dimensional Conjugated Oligomers with Anthracene as the Node. Chemistry - an Asian Journal, 2010, 5, 932-940.	3.3	15
192	Toward rational designing of n-type materials: Theoretical investigations of mer-Alq3 derivatives. Computational and Theoretical Chemistry, 2010, 956, 61-65.	1.5	15
193	Mechanism Study of the Intramolecular Anti-Michael Addition of <i>N</i> -Alkylfurylacrylacetamides. Journal of Organic Chemistry, 2012, 77, 8744-8749.	3.2	15
194	Construction of electrical "highway―to significantly enhance the redox kinetics of normal hierarchical structured materials of MnO. Journal of Materials Chemistry A, 2018, 6, 1663-1670.	10.3	15
195	Investigation on the mechanism of water-assisted palladium-catalyzed benzylic C–H amination by N-fluorobenzenesulfonimide. Organic and Biomolecular Chemistry, 2013, 11, 7923.	2.8	14
196	Theoretical investigations for organic solar cells. Materials Technology, 2013, 28, 40-64.	3.0	14
197	Multiscale simulation of pollution gases adsorption in porous organic cage CC3. Journal of Computational Chemistry, 2014, 35, 174-180.	3.3	14
198	Fabrication of both the photoactive layer and the electrode by electrochemical assembly: towards a fully solution-processable device. Chemical Communications, 2014, 50, 10448-10451.	4.1	14

#	Article	IF	CITATIONS
199	[DBUâ€H] <sup>+</sup> and H <sub>2</sub> 0 as effective catalyst form for 2,3â€dihydropyrido[2,3â€ <i>d</i> ]pyrimidinâ€4(1 <i>H</i> )â€ones: A DFT Study. Journal of Computational Chemistry, 2015, 36, 1295-1303.	3.3	14
200	An <i>in situ</i> â€Fabricated Composite Polymer Electrolyte Containing Largeâ€Anion Lithium Salt for Allâ€Solidâ€State LiFePO <sub>4</sub> /Li Batteries. ChemElectroChem, 2017, 4, 2293-2299.	3.4	14
201	Female nurses' burnout symptoms: No association with the Hypothalamic-pituitary-thyroid (HPT) axis. Psychoneuroendocrinology, 2017, 77, 47-50.	2.7	14
202	Selective chiral symmetry breaking and luminescence sensing of a Zn( <scp>ii</scp> ) metal–organic framework. Dalton Transactions, 2018, 47, 7934-7940.	3.3	14
203	In situ construction of ligand nano-network to integrin αvβ3 for angiogenesis inhibition. Chinese Chemical Letters, 2020, 31, 3107-3112.	9.0	14
204	Judicious design functionalized <scp>3D OF</scp> to enhance <scp>CO<sub>2</sub></scp> adsorption and separation. Journal of Computational Chemistry, 2021, 42, 888-896.	3.3	14
205	N-doped Porous Host with Lithiophilic Co Nanoparticles Implanted into 3D Carbon Nanotubes for Dendrite-Free Lithium Metal Anodes. ACS Applied Energy Materials, 2021, 4, 12871-12881.	5.1	14
206	DFT and TD-DFT investigation of the ground and excited states for dinuclear and mononuclear copper(I) and silver(I) complexes of 3,5-bis(trifluoromethyl)pyrazole and related bis(pyrazolyl)borate. Chemical Physics Letters, 2005, 410, 302-306.	2.6	13
207	Influence of the Substituted Side Group on the Molecular Structure and Electronic Properties of TPP and Related Implications on Organic Zeolites Use. Journal of Physical Chemistry B, 2007, 111, 5031-5033.	2.6	13
208	Theoretical Studies on the Magnetic Bistability of Dinickel Complex Tuned by Azide. Journal of Physical Chemistry A, 2008, 112, 3186-3191.	2.5	13
209	Adsorption of Gases in Microporous Organic Molecular Crystal, a Multiscale Computational Investigation. Journal of Physical Chemistry C, 2011, 115, 4935-4942.	3.1	13
210	[3+2] Cycloadditions of α-acyl ketene dithioacetals with propargylamines: pyrrole synthesis in water. Tetrahedron Letters, 2013, 54, 1478-1481.	1.4	13
211	The ratio and topology effects of benzodithiophene donor–benzooxadiazole acceptor fragments on the optoelectronic properties of donor molecules toward solar cell materials. Physical Chemistry Chemical Physics, 2015, 17, 7986-7999.	2.8	13
212	Theoretical studies to investigate the effect of different cores and two different topologies on the optical and charge transfer properties of donor materials for organic solar cells. New Journal of Chemistry, 2016, 40, 3693-3704.	2.8	13
213	Understanding the Mechanism of the Lewis Acid Promoted [3 + 2] Cycloaddition of Propargylic Alcohol and α-Oxo Ketene Dithioacetals. Journal of Organic Chemistry, 2016, 81, 1989-1997.	3.2	13
214	A Nano‣ized [Mn <sup>II</sup> <sub>18</sub> ] Metallamacrocycle as a Building Unit to Construct Stable Metal–Organic Frameworks: Effective Gas Adsorption and Magnetic Properties. Chemistry - A European Journal, 2018, 24, 19152-19155.	3.3	13
215	Charge control of the formation of two neutral/cationic metal–organic frameworks based on neutral/cationic triangular clusters and isonicotinic acid: structure, gas adsorption and magnetism. CrystEngComm, 2018, 20, 5402-5408.	2.6	13
216	Silver-promoted regio- and stereoselective aminocyanation of alkynes for the synthesis of β-aminoacrylonitriles using N-isocyanoiminotriphenylphosphorane. Tetrahedron Letters, 2019, 60, 1678-1681.	1.4	13

#	Article	IF	CITATIONS
217	Theoretical investigations of the realization of sky-blue to blue TADF materials <i>via</i> CH/N and H/CN substitution at the diphenylsulphone acceptor. Journal of Materials Chemistry C, 2019, 7, 6685-6691.	5.5	13
218	The Origin of the Reproduction of Different Nitrogen Uptakes in Covalent Organic Frameworks (COFs). Chemistry - A European Journal, 2019, 25, 2303-2312.	3.3	13
219	The ground state spin multiplicity of Schlenk-type biradicals and the influence of additional linkage to ladder type structures. Chemical Physics, 1996, 206, 339-351.	1.9	12
220	Theoretical design of blue emitting materials based on symmetric and asymmetric spirosilabifluorene derivatives. Theoretical Chemistry Accounts, 2008, 119, 489-500.	1.4	12
221	Two-step relaxation in the 3D spin-canted manganese phosphate with high P–O–Mn connectivity. Chemical Communications, 2011, 47, 1737-1739.	4.1	12
222	First principles investigation on the key factors of broad absorption spectra and electronic properties for oligothiophene and its derivatives for solar cells. International Journal of Quantum Chemistry, 2011, 111, 2089-2098.	2.0	12
223	Photophysical Properties of Phenyl- or Thiophene-Cored Branched Molecules with Thiophene and/or Thienylenevinylene Arms toward Broad Absorption Spectra for Solar Cells: A Theoretical Study. Journal of Physical Chemistry C, 2013, 117, 3221-3231.	3.1	12
224	Effect of length on the position of negative differential resistance and realization of multifunction in fused oligothiophenes based molecular device. Journal of Chemical Physics, 2013, 138, 074307.	3.0	12
225	Insights into Electrochemistry and Mechanical Stability of α- and β-Li <sub>2</sub> MnP <sub>2</sub> O <sub>7</sub> for Lithium-Ion Cathode Materials: First-Principles Comparison. Journal of Physical Chemistry C, 2017, 121, 22656-22664.	3.1	12
226	An "In Vivo Self-assembly―Strategy for Constructing Superstructures for Biomedical Applications. Chinese Journal of Polymer Science (English Edition), 2018, 36, 1103-1113.	3.8	12
227	Bifunctional Separator Coated with Hexachlorocyclotriphosphazene/Reduced Graphene Oxide for Enhanced Performance of Lithium–Sulfur Batteries. Chemistry - A European Journal, 2018, 24, 13582-13588.	3.3	12
228	Micro/Nanoengineered αâ€Fe 2 O 3 Nanoaggregate Conformably Enclosed by Ultrathin Nâ€Doped Carbon Shell for Ultrastable Lithium Storage and Insight into Phase Evolution Mechanism. Chemistry - A European Journal, 2020, 26, 853-862.	3.3	12
229	Two Metal–Organic Frameworks Based on Hexanuclear Cobalt–Hydroxyl Clusters or a Manganese–Hydroxyl Chain from Triangular [MII3(μ3-OH)] (M = Co and Mn) Units: Antiferromagnetic and Spin-Canting Antiferromagnetic Ordering with Soft-Magnetic Behavior. Inorganic Chemistry, 2020. 59. 12017-12024.	4.0	12
230	Psychological interventions for enhancing resilience in parents of children with cancer: a systematic review and meta-analysis. Supportive Care in Cancer, 2021, 29, 7101-7110.	2.2	12
231	Regulating Li nucleation/growth via implanting lithiophilic seeds onto flexible scaffolds enables highly stable Li metal anode. Journal of Colloid and Interface Science, 2022, 609, 606-616.	9.4	12
232	The stabilities of ground state multiplicities in triradicals and their dependence on configuration and conformation. Chemical Physics Letters, 1997, 269, 187-192.	2.6	11
233	Effect of configuration and conformation on the spin multiplicity in xylylene type biradicals. Science in China Series B: Chemistry, 2000, 43, 524-530.	0.8	11
234	Synthesis and Characterization of Monosubstituted TTF and Its Solvent Dependent Mono- and Dication Charge-Transfer Salts. Crystal Growth and Design, 2009, 9, 3855-3858.	3.0	11

#	Article	IF	CITATIONS
235	Designing of Disubstituted Derivatives of mer-Alq3: Quantum Theoretical Study. Australian Journal of Chemistry, 2010, 63, 1283.	0.9	11
236	Metallo‣upramolecular Nanogels for Intracellular pHâ€Responsive Drug Release. Macromolecular Rapid Communications, 2014, 35, 1697-1705.	3.9	11
237	Bis-pyrene carbocations for chromogenic and fluorogenic dual-detection of fluoride anion in situ. Tetrahedron, 2014, 70, 3172-3177.	1.9	11
238	Transition metal phosphite complexes: from one-dimensional chain, two-dimensional sheet, to three-dimensional architecture with unusual magnetic properties. CrystEngComm, 2014, 16, 1071-1078.	2.6	11
239	From Molecules to Materials: Computational Design of Nâ€Containing Porous Aromatic Frameworks for CO <sub>2</sub> Capture. ChemPhysChem, 2014, 15, 1772-1778.	2.1	11
240	Theoretical design and simulation of supramolecular polymer unit based on multiple hydrogen bonds. Journal of Molecular Graphics and Modelling, 2015, 59, 31-39.	2.4	11
241	A study of the electrochemical behavior at low temperature of the Li <sub>3</sub> V <sub>2</sub> (PO <sub>4</sub> ) <sub>3</sub> cathode material for Li-ion batteries. New Journal of Chemistry, 2015, 39, 9617-9626.	2.8	11
242	A stable luminescent zinc–organic framework as a dual-sensor toward Cu <sup>2+</sup> and Cr <sub>2</sub> O <sub>7</sub> <sup>2â^'</sup> , and excellent platform-encapsulated Ln <sup>3+</sup> for systematic color tuning and white-light emission. New Journal of Chemistry, 2019, 43, 13794-13801.	2.8	11
243	Covalent Organic Framework with Highly Accessible Carbonyls and π ation Effect for Advanced Potassiumâ€ion Batteries. Angewandte Chemie, 2022, 134, e202117661.	2.0	11
244	Role of Hydrogen Bonds in the Propagation of Ferromagnetic Coupling Between High Spin Molecules. Molecular Crystals and Liquid Crystals, 1997, 306, 119-123.	0.3	10
245	Energy decomposition analysis of methyl derivatives of the meridianal isomer of tris(8-hydroxyquinolino)aluminum (mer-Alq3). Chemical Physics, 2009, 358, 25-29.	1.9	10
246	Theoretical investigation of chemosensor for fluoride anion based on amidophthalimide derivatives. Theoretical Chemistry Accounts, 2009, 124, 225-234.	1.4	10
247	Theoretical investigation into optical and electronic properties of oligothiophene derivatives with phenyl ring as core or end-capped group in linear and V-shape. Theoretical Chemistry Accounts, 2011, 128, 165-174.	1.4	10
248	Reductive amination of tertiary anilines and aldehydes. Chemical Communications, 2013, 49, 8866.	4.1	10
249	Mechanism and kinetic study of 3-fluoropropene with hydroxyl radical reaction. Journal of Molecular Graphics and Modelling, 2014, 48, 18-27.	2.4	10
250	Silver-mediated radical coupling reaction of isocyanides and alcohols/phenols in the presence of water: unprecedented hydration and radical coupling reaction sequence. Organic and Biomolecular Chemistry, 2017, 15, 1580-1583.	2.8	10
251	Tuning the electronic and optical properties of diphenylsulphone based thermally activated delayed fluorescent materials via structural modification: A theoretical study. Dyes and Pigments, 2017, 143, 42-47.	3.7	10
252	Insight into electrochemical and elastic properties in AFe1-M SO4F (A = Li, Na; M = Co, Ni, Mg) cathode materials: A first principle study. Electrochimica Acta, 2017, 251, 316-323.	5.2	10

#	Article	IF	CITATIONS
253	Reversible adsorption/desorption of the formaldehyde molecule on transition metal doped graphene by controlling the external electric field: first-principles study. Theoretical Chemistry Accounts, 2017, 136, 1.	1.4	10
254	Tetranuclear cobalt( <scp>ii</scp> )–isonicotinic acid frameworks: selective CO <sub>2</sub> capture, magnetic properties, and derived "Co <sub>3</sub> O <sub>4</sub> ―exhibiting high performance in lithium ion batteries. Dalton Transactions, 2019, 48, 296-303.	3.3	10
255	<i>In Situ</i> Growth of 3D Lamellar Mn(OH) <sub>2</sub> on CuO-Coated Carbon Cloth for Flexible Asymmetric Supercapacitors with a High Working Voltage of 2.4 V. ACS Sustainable Chemistry and Engineering, 2021, 9, 13385-13394.	6.7	10
256	Synthesis of poly(phenylenesulfidephenylenamine) by self-polycondensation of methyl-(4-anilinophenyl) sulfide with antimony pentachloride. Synthetic Metals, 1999, 101, 320.	3.9	9
257	Design of TTF-Based Phosphazenes Combining a Good Electron-Donor Capacity and Possible Inclusion Adduct Formation. Journal of Physical Chemistry B, 2006, 110, 16852-16859.	2.6	9
258	Structural and magnetic properties of metal complexes with pyridine-2,6-dicarboxylate and 5-(4-bromophenyl)-2,4′-bipyridine. Polyhedron, 2009, 28, 980-986.	2.2	9
259	The correlation between magnetism and structures for new solvent free iron(III) and chromium(III) homoleptic 8-quinolinato complexes. Inorganica Chimica Acta, 2011, 366, 241-246.	2.4	9
260	Polypyrrole nanosphere embedded in wrinkled graphene layers to obtain cross-linking network for high performance supercapacitors. Electrochimica Acta, 2015, 184, 179-185.	5.2	9
261	Computational design of benzo [1,2-b:4,5-b′] dithiophene based thermally activated delayed fluorescent materials. Dyes and Pigments, 2016, 127, 189-196.	3.7	9
262	Interruption of Formal Schmidt Rearrangement/Hosomi–Sakurai Reaction of Vinyl Azides with Allyl/Propargylsilanes. Organic Letters, 2018, 20, 7113-7116.	4.6	9
263	A computational mechanistic study of substrate-controlled competitive O–H and C–H insertion reactions catalyzed by dirhodium( <scp>ii</scp> ) carbenoids: insight into the origin of chemoselectivity. Organic Chemistry Frontiers, 2018, 5, 2353-2363.	4.5	9
264	The effect of CF3 functional group substituent on bifunctional activation model and enantioselectivity for BINOL N-triflylphosphoramides catalyzed rearrangement reaction. Journal of Catalysis, 2020, 383, 230-238.	6.2	9
265	Intramolecular Exchange Interaction in Xylylene Type Biradicals. Molecular Crystals and Liquid Crystals, 1997, 305, 509-514.	0.3	8
266	The effective position of radical substitution on pyridine ligands for the exchange interaction in 1:2 complexes of paramagnetic ion and organic radicals: a DFT study. Synthetic Metals, 2003, 137, 1355-1356.	3.9	8
267	Mass transfer resistance in the production of high impact polypropylene. Polymer, 2008, 49, 2974-2978.	3.8	8
268	Structural and magnetic property of one-dimensional polymeric Ni(II) complex. Journal of Molecular Structure, 2008, 873, 191-194.	3.6	8
269	Two unique 8-quinolinato (q) based one dimensional complexes [Fe <sup>II</sup> Mn <sup>II</sup> (q) <sub>4</sub> ·(H <sub>2</sub> O) <sub>0.25</sub> ] <sub>n</sub> and [Mn <sup>II</sup> (q) <sub>2</sub> ] <sub>n</sub> : synthesis, structures, and magnetism. CrystEngComm. 2011. 13. 418-420.	2.6	8
270	Mechanistic and kinetic study the reaction of O(3P)Â+ÂCH3CFCH2. Theoretical Chemistry Accounts, 2012, 131, 1.	1.4	8

#	Article	IF	CITATIONS
271	Hierarchicallyâ€Porous Carbon Derived from a Largeâ€6cale Ironâ€based Organometallic Complex for Versatile Energy Storage. ChemSusChem, 2016, 9, 1483-1489.	6.8	8
272	DFT studies on the mechanism of Ag <sub>2</sub> CO <sub>3</sub> â€catalyzed hydroazidation of unactivated terminal alkynes with TMSâ€N <sub>3</sub> : An insight into the silver(I) activation mode. Journal of Computational Chemistry, 2017, 38, 2289-2297.	3.3	8
273	Micron-scaled MoS2/N-C particles with embedded nano-MoS2: A high-rate anode material for enhanced lithium storage. Applied Surface Science, 2019, 486, 519-526.	6.1	8
274	Assembly of metal–organic frameworks based on 4-connected 3,3′,5,5′-azobenzenetetracarboxylic acid: structures, magnetic properties, and sensing of Fe <sup>3+</sup> ions. New Journal of Chemistry, 2019, 43, 4226-4234.	2.8	8
275	Impact of WeChatâ€based 'three good things' on turnover intention and coping style in burnout nurses. Journal of Nursing Management, 2020, 28, 1570-1577.	3.4	8
276	Pseudocapacitive Lithium Storage of Cauliflowerâ€Like CoFe <sub>2</sub> O <sub>4</sub> for Lowâ€Temperature Battery Operation. Chemistry - A European Journal, 2020, 26, 13652-13658.	3.3	8
277	Insights into the Chiral Phosphoric Acid-Catalyzed Dynamic Kinetic Asymmetric Hydroamination of Racemic Allenes: An Allyl Carbocation/Phosphate Pair Mechanism. Journal of Organic Chemistry, 2021, 86, 4121-4130.	3.2	8
278	Robust Electrodes for Flexible Energy Storage Devices Based on Bimetallic Encapsulated Core–Multishell Structures. Advanced Science, 2021, 8, e2100911.	11.2	8
279	A Poreâ€Forming Strategy Toward Porous Carbonâ€Based Substrates for High Performance Flexible Lithium Metal Full Batteries. Energy and Environmental Materials, 2023, 6, .	12.8	8
280	Uniform Zn <sup>2+</sup> Flux Distribution Achieved by an Artificial Three-Dimensional Framework: The Enhanced Ion-Transfer Kinetics for Long-Life and Dendrite-Free Zn Anodes. ACS Applied Materials & Interfaces, 2022, 14, 23558-23569.	8.0	8
281	Theoretical design of high-spin organic molecules with two-center, three-electron spin-containing units. Journal of Physical Organic Chemistry, 1999, 12, 53-60.	1.9	7
282	DFT investigation for 1:2 complexes of bis(hexafluoroacetylacetonato)copper(II) coordinated with 4-(N-tert-butyl-N-oxyamino)pyridine. Polyhedron, 2007, 26, 2126-2128.	2.2	7
283	Solvothermal synthesis, structure, and magnetic property for nano-â€ <sup>~</sup> chromic wheels' [Cr10(μ-O2CMe)10(μ-OMe)10(μ-OEt)10]. Polyhedron, 2007, 26, 2169-2173.	2.2	7
284	Combined Effects of One 8-Hydroxyquinoline/Picolinate and "CHâ€ <b>/</b> N Substitutions on the Geometry, Electronic Structure and Optical Properties of <i>mer</i> -Alq <sub>3</sub> . Journal of Physical Chemistry A, 2010, 114, 652-658.	2.5	7
285	Optical and transport properties of single crystal rubrene: A theoretical study. Chemical Physics, 2016, 481, 198-205.	1.9	7
286	4-Dimethylaminopyridine-catalyzed dynamic kinetic resolution in asymmetric synthesis of P-chirogenic 1,3,2-oxazaphospholidine-2-oxides. RSC Advances, 2016, 6, 89665-89670.	3.6	7
287	Mechanistic insights on DBU catalyzed <i>β</i> â€emination of nbs to chalcone driving by water: Multiple roles of water. Journal of Computational Chemistry, 2017, 38, 438-445.	3.3	7
288	Theoretical simulation of CO <sub>2</sub> capture in organic cage impregnated with polyoxometalates. Journal of Computational Chemistry, 2017, 38, 612-619.	3.3	7

#	Article	IF	CITATIONS
289	Mechanistic Insights into the Nickel-Catalyzed Cross-Coupling Reaction of Benzaldehyde with Benzyl Alcohol via C–H Activation: A Theoretical Investigation. Journal of Organic Chemistry, 2018, 83, 11905-11916.	3.2	7
290	Chiral Phosphoric Acid-Catalyzed Enantioselective Direct Arylation of Iminoquinones: A Case Study of the Model Selectivity. Journal of Organic Chemistry, 2019, 84, 13473-13482.	3.2	7
291	Theoretical Investigation of the Topology of Spiroborate‣inked Ionic Covalent Organic Frameworks (ICOFs). Chemistry - A European Journal, 2019, 25, 6569-6574.	3.3	7
292	The control effects of different scaffolds in chiral phosphoric acids: a case study of enantioselective asymmetric arylation. Catalysis Science and Technology, 2019, 9, 6482-6491.	4.1	7
293	Understanding the electrochemical properties of bulk phase and surface structures of Na <sub>3</sub> T <sup>M</sup> PO <sub>4</sub> CO <sub>3</sub> (T <sup>M</sup> = Fe, Mn, Co, Ni) from first principles calculations. Physical Chemistry Chemical Physics, 2020, 22, 25325-25334.	2.8	7
294	Sustainable and Robust Graphene Cellulose Paper Decorated with Lithiophilic Au Nanoparticles to Enable Dendriteâ€free and Highâ€Power Lithium Metal Anode. Chemistry - A European Journal, 2021, 27, 8168-8177.	3.3	7
295	Pseudocapacitive sodium storage in a new brand foveolate TiO <sub>2</sub> @MoSe <sub>2</sub> nanocomposite for high-performance Na-ion hybrid capacitors. Journal of Materials Chemistry A, 2021, 9, 24419-24425.	10.3	7
296	Using triazine as coupling unit for intramolecular ferromagnetic coupling of multiradicals. Chemical Physics, 1999, 246, 209-215.	1.9	6
297	Theoretical study of tris(o-phenylenedioxy) cyclotrisphosphazene (TPP) electronic structure with ab initio and DFT methods. Chemical Physics Letters, 2004, 388, 422-426.	2.6	6
298	Theoretical investigation of magnetic properties of a heterospin system consisting of manganese(II) [Mn(hfac)2(4NOPy)2]: A broken symmetry approach combined with density functional theory. Computational and Theoretical Chemistry, 2008, 867, 33-38.	1.5	6
299	Photophysical Properties of Derivatives of 2-(2-Hydroxyphen-yl)-1,3,4-oxadiazole: A Theoretical Study. Journal of Physical Chemistry A, 2013, 117, 8285-8292.	2.5	6
300	Li <sub>2</sub> FePO <sub>4</sub> F and its metal-doping for Li-ion batteries: an ab initio study. RSC Advances, 2014, 4, 50195-50201.	3.6	6
301	Study on fluorescent switching of naphthopyran with carbazole and pyrene dyad immobilized on SBA-15. Tetrahedron, 2014, 70, 5966-5973.	1.9	6
302	Modeling the selectivity of indoor pollution gases over N2 on covalent organic frameworks. Journal of Molecular Modeling, 2014, 20, 2346.	1.8	6
303	The multieffects of DMF and DBU on the [5 + 1] benzannulation of nitroethane and αâ€alkenoyl keteneâ€( <i>S,S</i> )â€acetals: Hydrogen bonding and electrostatic interactions. Journal of Computational Chemistry, 2015, 36, 731-738.	3.3	6
304	Mechanistic insight on ( <i>E</i> )â€methyl 3â€(2â€aminophenyl)acrylate cyclization reaction by multicatalysis of solvent and substrate. Journal of Computational Chemistry, 2016, 37, 2386-2394.	3.3	6
305	Theoretical Simulation of CH <sub>4</sub> Separation from H <sub>2</sub> in CAU-17 Materials. Journal of Physical Chemistry C, 2017, 121, 20197-20204.	3.1	6
306	<i>In situ</i> chemically encapsulated and controlled SnS <sub>2</sub> nanocrystal composites for durable lithium/sodium-ion batteries. Dalton Transactions, 2020, 49, 15874-15882.	3.3	6

#	Article	IF	CITATIONS
307	A Trinuclear Cobalt–Organic Framework: Solvatochromic Sensor towards CH <sub>2</sub> Cl <sub>2</sub> , and its Derivative as an Anode of Lithiumâ€Ion Batteries with High Performance. Chemistry - A European Journal, 2020, 26, 14187-14193.	3.3	6
308	Ab initio study for the effect of hydrogen bonds in the intermolecular interaction between high-spin molecules. Synthetic Metals, 2003, 137, 1349-1350.	3.9	5
309	Broken symmetry approach and density functional theory investigation on hetero-spin system consisting of copper(II) and aminoxyl radicals: Comparison and reliability of different basis sets approaches. Computational and Theoretical Chemistry, 2009, 896, 54-62.	1.5	5
310	Structural and magnetic properties of 1D coordination polymers constructed by isophthalate and 2,4′-bipyridine. Journal of Molecular Structure, 2009, 927, 21-26.	3.6	5
311	The Origin of the High Enantioselectivity in Asymmetric Cyclopropanation of Unfunctionalized Olefins. Advanced Synthesis and Catalysis, 2010, 352, 1810-1817.	4.3	5
312	Electronic structures and optical properties of the IPR-violating C60X8 (X = H, F, and Cl) fullerene compounds: a computational study. Physical Chemistry Chemical Physics, 2012, 14, 16476.	2.8	5
313	Theoretical study on the gas phase reaction of allyl chloride with hydroxyl radical. Journal of Chemical Physics, 2014, 140, 084309.	3.0	5
314	Gas adsorption in Mgâ€porphyrinâ€based porous organic frameworks: A computational simulation by firstâ€principles derived force field. Journal of Computational Chemistry, 2017, 38, 2100-2107.	3.3	5
315	<i>In situ</i> construction of nanonetworks from transformable nanoparticles for anti-angiogenic therapy. Journal of Materials Chemistry B, 2018, 6, 5282-5289.	5.8	5
316	Targeted Construction of Amorphous MoS <sub><i>x</i></sub> with an Inherent Chain Molecular Structure for Improved Pseudocapacitive Lithiumâ€ion Response. Chemistry - A European Journal, 2019, 25, 15173-15181.	3.3	5
317	2D Metalâ€Organic Framework Derived Co 3 O 4 for the Oxygen Evolution Reaction and Highâ€Performance Lithiumâ€Ion Batteries. ChemNanoMat, 2020, 6, 1770-1775.	2.8	5
318	Mechanistic Study on Ag <sup>I</sup> -Catalyzed Oxidative Cross-Coupling/Cyclization between Terminal Alkynes and β-Enamino Esters under Base Conditions. Journal of Organic Chemistry, 2020, 85, 4408-4417.	3.2	5
319	Mechanistic details of metalâ€free cyclization reaction of organophosphorus oxide with alkynes mediated by 2,6â€lutidine and Tf 2 O. Journal of Computational Chemistry, 2020, 41, 1709-1717.	3.3	5
320	Poly[pentakis(μ-cyanido-β <sup>2</sup> <i>N</i> : <i>C</i> )tris(5-phenyl-2,2â€2-bipyridine-β <sup>2</sup> <i>Acta Crystallographica Section E: Structure Reports Online, 2011, 67, m1706-m1707.</i>	NN	′)penta
321	Theoretical investigation of the chemical bonds in metal chelates as emitting material for OLED. Synthetic Metals, 2005, 152, 241-244.	3.9	4
322	Hydrogen-bonded Lamellar Network of Pyromellitic Acid Pillared by 8-Hydroxyquinoline. Chinese Journal of Chemistry, 2006, 24, 573-576.	4.9	4
323	Substituent effects in the tuning of excited-state intramolecular proton transfer and optical properties of the derivatives of 2-(2-hydroxyphenyl)-5-phenyl-1,3,4-oxadiazole. Theoretical Chemistry Accounts, 2009, 124, 331-338.	1.4	4
324	Computational study of oxygen atom (3P and 1D) reactions with CF3CN. Physical Chemistry Chemical Physics, 2010, 12, 10846.	2.8	4

#	Article	IF	CITATIONS
325	Encapsulated different forms of water molecules by Cu(ii) complexes with diverse structures. CrystEngComm, 2010, 12, 2734.	2.6	4
326	The low spin Coll fragment with homoleptic 1,10-phenanthroline ligands: synthesis, structures, DFT investigations, and magnetic properties. Dalton Transactions, 2011, 40, 4459.	3.3	4
327	Exploration of the slow relaxation behavior in the manganese phosphate network. Dalton Transactions, 2014, 43, 9267-9270.	3.3	4
328	The mechanistic study of the hydroxyl radical reaction with trans-2-chlorovinyldichloroarsine. Journal of Molecular Modeling, 2014, 20, 2335.	1.8	4
329	Mechanistic investigation on N → C <sup>α</sup> → O relay via non-Brook rearrangement: reaction conditions promote synthesis of furo[3,2-c]pyridinones. Organic and Biomolecular Chemistry, 2017, 15, 9127-9138.	2.8	4
330	Mechanistic investigation inspired "on water†reaction for hydrobromic acidâ€catalyzed Friedel–Crafts–type reaction of <i>î²</i> â€naphthol and formaldehyde. Journal of Computational Chemistry, 2017, 38, 2268-2275.	3.3	4
331	A mechanistic investigation into N-heterocyclic carbene (NHC) catalyzed umpolung of ketones and benzonitriles: is the cyano group better than the classical carbonyl group for the addition of NHC?. Organic Chemistry Frontiers, 2019, 6, 523-531.	4.5	4
332	Boron-doped Sb/SbO <sub>2</sub> @rGO composites with tunable components and enlarged lattice spacing for high-rate sodium-ion batteries. Journal Physics D: Applied Physics, 2021, 54, 315505.	2.8	4
333	Quasi-Grotthuss mechanism in a nonporous sulphate. Journal of Energy Chemistry, 2021, 57, 233-237.	12.9	4
334	Enantioselective synthesis of chiral tetrasubstituted allenes: harnessing electrostatic and noncovalent interactions in a bifunctional activation model for <i>N</i> -triflylphosphoramide catalysis. Organic Chemistry Frontiers, 2021, 8, 1510-1519.	4.5	4
335	Design of high-spin molecules incorporating charged plus neutral spin centers. Heteroatom Chemistry, 1998, 9, 161-167.	0.7	3
336	Dependence of multiplicity on conformation: ground states of o-, m- and p-phenylenediamine dications. Synthetic Metals, 1999, 100, 261-268.	3.9	3
337	Theoretical Study of Unsymmetrical Bisfullerene and Its Derivatives:Â C131, C129BN, and C130Si. Journal of Physical Chemistry A, 2006, 110, 9921-9926.	2.5	3
338	Synthesis, crystal structure and magnetic properties of a new 30 cobalt vanadate. Chinese Journal of Chemistry, 2004, 22, 638-641.	4.9	3
339	The magneto-structural correlation of two novel 1D antiferromagnetic chains with different magnetic behaviors. Polyhedron, 2011, 30, 3100-3105.	2.2	3
340	Theoretical study on the mechanism for the reaction of OH with CH2CHCH(OH)CH3. Computational and Theoretical Chemistry, 2011, 965, 68-83.	2.5	3
341	Rapid α-Amination of N-Substituted Indoles by Using DBU-Activated N-Haloimides as Nitrogen Sources. Synlett, 2014, 26, 116-122.	1.8	3
342	Double Carbon Nano Coating of LiFePO <sub>4</sub> Cathode Material for High Performance of Lithium Ion Batteries. Journal of Nanoscience and Nanotechnology, 2015, 15, 9630-9635.	0.9	3

#	Article	IF	CITATIONS
	Solvothermal synthesis, crystal structures and characterization of open-framework metal (Coll and) Tj ETQq1 1 0		<u> </u>
343	2017, 84, 77-80.	3.9	3
344	Selective CO <sub>2</sub> adsorption and theoretical simulation of a stable Co( <scp>ii</scp> )-based metal–organic framework with tunable crystal size. CrystEngComm, 2019, 21, 1564-1569.	2.6	3
345	A novel emitting polymer with bipolar carrier transporting abilities. Journal of Applied Polymer Science, 2003, 88, 50-53.	2.6	2
346	Bis(2,4′-bipyridin-1′-ium) 2,5-dicarboxybenzene-1,4-carboxylate benzene-1,2,4,5-tetracarboxylic acid. Acta Crystallographica Section E: Structure Reports Online, 2005, 61, o2193-o2195.	0.2	2
347	Redetermination of poly[î¼2-aqua-diaquabis(î¼3-pyridine-2,6-dicarboxylato)manganese(II)]. Acta Crystallographica Section E: Structure Reports Online, 2007, 63, m3102-m3102.	0.2	2
348	Modulation of Tris(o-phenylenedioxy)cyclotrisphosphazene (TPP) Properties for Zeolite Use: Effect of Ï€-Conjugation Length and CH/N Heterosubstitution. Journal of Physical Chemistry A, 2009, 113, 246-254.	2.5	2
349	Design of tetrathiafulvalene-based TPP analogues combining a good electron-donor capacity and a possible organic zeolite formation: A computational investigation. Computational and Theoretical Chemistry, 2010, 940, 13-18.	1.5	2
350	An asymmetric TTF derivative bearing a phenyl β-diketone group as an efficient ligand towards functional materials. New Journal of Chemistry, 2011, 35, 1472.	2.8	2
351	<i>catena</i> -Poly[[(5-phenyl-2,2′-bipyridine-l̂° <sup>2</sup> <i>N</i> , <i>N</i> ′)copper(I)]-l̂¼-thiocyanido- Acta Crystallographica Section E: Structure Reports Online, 2012, 68, m165-m165.	<sup>°</sup> ² <sup>2∢ 0.2</sup>	syb> <i>N&lt;</i>
352	Anchor position and donor/acceptor effects on transport properties in fused benzene-substituted oligothiophene molecular device. Physica E: Low-Dimensional Systems and Nanostructures, 2013, 54, 247-252.	2.7	2
353	Mechanistic and kinetic study on the reaction of ozone and trans-2-chlorovinyldichloroarsine. Chemosphere, 2016, 150, 329-340.	8.2	2
354	Simulations of Gas Adsorption in Thiophene-Based Cyclo-1,4-phenylene-2′,5′-thienylenes Using First-Principles-derived Force Field. Journal of Physical Chemistry C, 2016, 120, 4329-4336.	3.1	2
355	Mechanistic insights into Nâ€Bromosuccinimideâ€promoted synthesis of imidazo[1,2â€∢i>a]pyridine in water: Reactivity mediated by substrates and solvent. Journal of Computational Chemistry, 2018, 39, 2324-2332.	3.3	2
356	Mechanistic investigation-inspired activation mode of DBU and the function of the α-diazo group in the reaction of the α-amino ketone compound and EDA: [DBU-H] <sup>+</sup> -DMF-H <sub>2</sub> O and α-diazo as strong N-terminal nucleophiles. Organic Chemistry Frontiers, 2019, 6, 2678-2686.	4.5	2
357	Comparison of Reliability and Validity of the Chinese Four-Level and Three-District Triage Standard and the Australasian Triage Scale. Emergency Medicine International, 2019, 2019, 1-8.	0.8	2
358	CO oxidation on atomic nickel/phosphorene nanosheet: An efficient single-atom catalyst. Molecular Catalysis, 2021, 510, 111626.	2.0	2
359	First-principles study of borophene/phosphorene heterojunction as anode material for lithium-ion batteries. Nanotechnology, 2022, 33, 075403.	2.6	2
360	The intermolecular coupling through space for stacked high spin molecules. Synthetic Metals, 1999, 103, 2273-2274.	3.9	1

#	Article	IF	CITATIONS
361	Theoretical Study on the Exchange Interaction Between Metal Ion and Organic Radical Through Pyridine, Bipyridine and Terpyridine Ligands. Molecular Crystals and Liquid Crystals, 2002, 376, 431-436.	0.9	1
362	α,α-Diacetyl Cyclic Ketene Dithioacetals: Odorless and Efficient Dithiol Equivalents in Thioacetalization Reactions. Synlett, 2004, 2004, 999-1002.	1.8	1
363	4,4',5,5'-Tetrakis(methylsulfanyl)tetrathiafulvalene. Acta Crystallographica Section E: Structure Reports Online, 2005, 61, o65-o66.	0.2	1
364	Bis[tetrakis(methylsulfanyl)tetrathiafulvalenium] oxalate dichloride. Acta Crystallographica Section E: Structure Reports Online, 2005, 61, o1674-o1676.	0.2	1
365	Structural and magnetic properties of metal complexes constructed by pyridine-2,6-dicarboxylate and 5-(4-bromophenyl)-2,4′-bipyridine. Synthetic Metals, 2009, 159, 2191-2193.	3.9	1
366	Theoretical study of the excited-state intramolecular proton transfer and rotamerism in 2,5-bis(2-hydroxyphenyl)-1,3,4-oxadiazole. Theoretical Chemistry Accounts, 2010, 126, 351-360.	1.4	1
367	Theoretical study on the mechanism for the reaction of F with CH2CHCH2Cl. Computational and Theoretical Chemistry, 2012, 981, 7-13.	2.5	1
368	Frontispiz: Covalent Organic Framework with Highly Accessible Carbonyls and π ation Effect for Advanced Potassiumâ€lon Batteries. Angewandte Chemie, 2022, 134, .	2.0	1
369	Theory study on conduction mechanism of polyphenothiazine and the possibility of its double doping. Synthetic Metals, 1991, 43, 3399-3402.	3.9	0
370	Novel Highly Selective Anion Chemosensors Based on 2,5-Bis(2-hydroxyphenyl)-1,3,4-oxadiazole ChemInform, 2003, 34, no.	0.0	0
371	The First Nonthiolic, Odorless 1,3-Propanedithiol Equivalent and Its Application in Thioacetalization ChemInform, 2004, 35, no.	0.0	0
372	catena-Poly[[[bis(2-pyridinecarboxylato-lº2N,O)copper(II)]-l̂¼-benzene-1,2,4,5-tetracarboxylic acid] dihydrate]. Acta Crystallographica Section E: Structure Reports Online, 2005, 61, m958-m960.	0.2	0
373	Theoretical Design of High-spin Organic Molecules with Ë™ NS as a Spin-containing Fragment and Heterocycle as End Groups1. Chemical Research in Chinese Universities, 2006, 22, 631-634.	2.6	0
374	Application of Density Functional Theoretic Descriptors to Quantitative Structure-Activity Relationships with Temperature Constrained Cascade Correlation Network Models of Nitrobenzene Derivatives1. Chemical Research in Chinese Universities, 2006, 22, 439-442.	2.6	0
375	Theoretical Design of High-spin Organic Molecules with —·N—N— as a Spin-containing Fragment and Heterocycles as an End Group. Chinese Journal of Chemistry, 2006, 24, 1648-1652.	4.9	0
376	Effects of Azido Bridge on Magnetic Properties of Dinuclear Nickel Complexes: Density Functional Theory Studies. Wuli Huaxue Xuebao/ Acta Physico - Chimica Sinica, 2015, 31, 1086-1092.	4.9	0
377	Reply to Letter to the Editor: Below is our response to the concerns raised by Dr. Bianchi et al. regarding our manuscript (Guo, Y., Lam, L., Luo, Y., Plummer, V., Cross, W., Li, H., Yin, Y., Zhang, J., 2017.) Tj ETQq	1 <u>1 0</u> .784 2.7	-314 rgBT /C
970	Mechanistic insight on water and substrate catalyzed the synthesis of		of0

378 3â€(1<i>H</i>à€indolâ€3â€yl)â€2â€(4â€methoxybenzyl)isoindolinâ€1â€one: Driving by noncovalent interactions.3@urnal ofo Computational Chemistry, 2018, 39, 2316-2323.

#	Article	IF	CITATIONS
379	Identifying a Clinical Risk Triage Score for Adult Emergency Department. Clinical Nursing Research, 2021, 30, 1135-1143.	1.6	0
380	New High-Nuclear Coordination Complexes Constructed by 2-Hydroxymethylpyridine: From Antiferromagnetic to Spin Glass and Ferromagnetic Behavior. Crystal Growth and Design, 2021, 21, 2754-2762.	3.0	0
381	The Design of Blue Emitting Materials Based on Spirosilabifluorene Derivatives. Lecture Notes in Computer Science, 2007, , 319-326.	1.3	0
382	Energy Partitioning Analysis of the Chemical Bonds in mer-Mq3 (M = AlIII, GalII, InIII, TIIII). Lecture Notes in Computer Science, 2007, , 331-334.	1.3	0
383	The Design of Tris(o-phenylenedioxy)cyclo-trisphosphazene (TPP) Derivatives and Analogs toward Multifunctional Zeolite Use. Lecture Notes in Computer Science, 2009, , 229-237.	1.3	0
384	Theoretical Study on the Exchange Interaction Between Metal Ion and Organic Radical Through Pyridine, Bipyridine and Terpyridine Ligands. Molecular Crystals and Liquid Crystals, 2002, 376, 431-436.	0.3	0